Xe NMR Chemical Shift in Xe@C 60 Calculated at Experimental Conditions: Essential Role of the Relativity, Dynamics, and Explicit Solvent

DATASET · JANUARY 2013

READS
29

4 AUTHORS, INCLUDING:

Radek Marek
Masaryk University
126 PUBLICATIONS **1,727** CITATIONS
SEE PROFILE

Michal Straka
Academy of Sciences of the Czech Republic
62 PUBLICATIONS **1,019** CITATIONS
SEE PROFILE

^{129}Xe NMR Chemical Shift in Xe@C_{60} Calculated at Experimental Conditions: Essential Role of the Relativity, Dynamics, and Explicit Solvent

Stanislav Standara,[a,c] Petr Kulhánek,[b,c] Radek Marek,[b,c] and Michal Straka*[a,b]

The isotropic ^{129}Xe nuclear magnetic resonance (NMR) chemical shift (CS) in Xe@C_{60} dissolved in liquid benzene was calculated by piecewise approximation to faithfully simulate the experimental conditions and to evaluate the role of different physical factors influencing the ^{129}Xe NMR CS. The ^{129}Xe shielding constant was obtained by averaging the ^{129}Xe nuclear magnetic shieldings calculated for snapshots obtained from the molecular dynamics trajectory of the Xe@C_{60} system embedded in a periodic box of benzene molecules. Relativistic corrections were added at the Breit–Pauli perturbation theory (BPPT) level, included the solvent, and were dynamically averaged. It is demonstrated that the contribution of internal dynamics of the Xe@C_{60} system represents about 8% of the total nonrelativistic NMR CS, whereas the effects of dynamical solvent add another 8%. The dynamically averaged relativistic effects contribute by 9% to the total calculated ^{129}Xe NMR CS. The final theoretical value of 172.7 ppm corresponds well to the experimental ^{129}Xe CS of 179.2 ppm and lies within the estimated errors of the model. The presented computational protocol serves as a prototype for calculations of ^{129}Xe NMR parameters in different Xe atom guest–host systems. © 2013 Wiley Periodicals, Inc.

DOI: 10.1002/jcc.23334

Introduction

Xe atom is an excellent nuclear magnetic resonance (NMR) probe due to its large and polarizable electron cloud. The electronic environment of the Xe atom and its time modulation are sensitively reflected in the NMR parameters of the ^{129}Xe nucleus, such as the NMR chemical shift (CS), chemical shift anisotropy, and NMR relaxation rates. The large polarizability of electron cloud is recoded in a broad range of ^{129}Xe NMR CSs spanning several thousands of ppm in Xe chemical compounds[1] and several hundreds of ppm in Xe atom guest–host materials.[2]

Chemical inertness allows the Xe atom to enter different materials without reacting chemically. The ^{129}Xe NMR spectroscopy thus provides a unique tool for studying various materials and their properties. This includes studies of ordering and dynamics in liquid crystals,[3,4] solvent dynamics in liquids,[5,6] structure of porous solids,[7,8] polymers,[9,10] and clathrates.[11,12] Glasses,[13] metallo-organic frameworks,[14,15] and crystals[16] have been also studied by means of ^{129}Xe NMR. Magnetic resonance imaging (MRI) studies based on ^{129}Xe NMR use biosensors in which the ^{129}Xe atom is confined in a molecular cage, such as cryptophane.[17–29]

Although the experimental studies provide the most important information about the phase transitions, pore sizes, or macroscopic structure of the studied materials, computations may help in understanding the situations at the microscopic level, resolving the experimental and theoretical questions, and providing the predictions for different real or hypothetical situations. Numerous computational studies on ^{129}Xe NMR properties have been reported for molecules containing Xe[30–35] as well as for Xe atom guest–host systems.[33,36–50]

In this article, we study the ^{129}Xe CS of endohedral Xe atom in Xe@C_{60} molecule with particular aim at faithful simulations of experimental conditions and assessment of the different physical contributions to the experimental ^{129}Xe NMR CS, such as relativistic, dynamic, and solvent effects.

Xe@C_{60} is a single-molecule prototype of confined Xe guest–host system (Fig. 1). It was first time prepared by exposing the C_{60} fullerene to Xe gas at 3000 atm and 650 K. The ^{129}Xe NMR signal of this system was measured to be 179.2 ppm in benzene using Xe gas at 1 atm as reference.[51]

Several theoretical studies on ^{129}Xe CS in Xe@C_{60} have been published. Bühl et al.[38] obtained a value of 71.7 ppm for the ^{129}Xe shift at the Hartree–Fock nonrelativistic level. Sears and Jameson[39] using nonrelativistic (NR) approximation and B3LYP functional in equilibrium geometry calculations obtained an excellent agreement with the experiment.

[a] S. Standara, M. Straka
Institute of Organic Chemistry and Biochemistry, Academy of Sciences of the Czech Republic, Flemingovo nám. 2, Praha 6, CZ-16610, Czech Republic
E-mail: straka@uochb.cas.cz
[b] P. Kulhánek, R. Marek, M. Straka
CEITEC—Central European Institute of Technology, Masaryk University, Kamenice 5/A4, CZ-62500, Brno, Czech Republic
[c] S. Standara, P. Kulhánek, R. Marek
Faculty of Science, National Center for Biomolecular Research, Masaryk University, Kamenice 5, CZ-62500, Brno, Czech Republic

Contract grant sponsor: Czech Academy of Sciences; Contract grant number: RVO 61388963; Contract grant sponsor: Ministry of Education, Youth, and Sports of the Czech Republic; Contract grant sponsor: Czech Science Foundation; Contract grant number: 203/09/2037 and 13-03978S; Contract grant sponsor: "CEITEC—Central European Institute of Technology" (European Regional Development); Contract grant number: CZ.1.05/1.1.00/02.0068; Contract grant sponsor: 7th European Community Framework Program (P.K.); Contract grant number: 286154

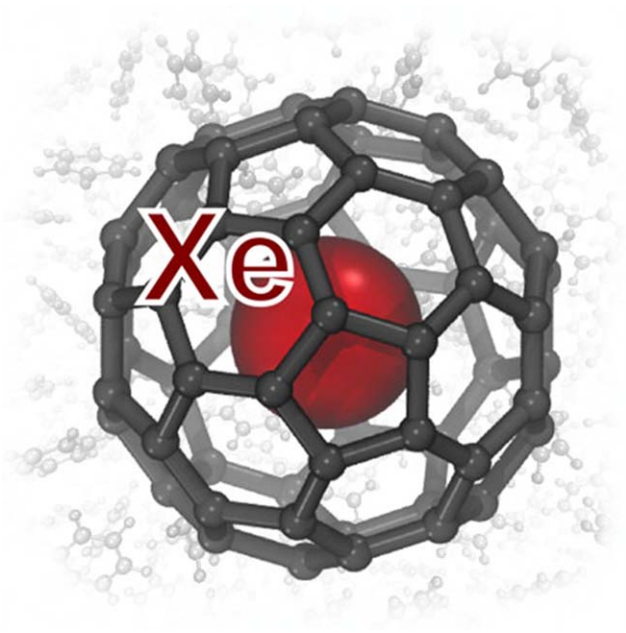

Figure 1. Xe@C_{60} dissolved in benzene. [Color figure can be viewed in the online issue, which is available at wileyonlinelibrary.com]

Autschbach and Zurek[37] used the zeroth-order relativistic approximation density functional theory (DFT) approach in a careful investigation of the methodological aspects of the problem, including the basis set limit, choice of the exchange-correlation functional, role of the relativistic effects, and a rough estimate of the role of the dynamics of the Xe atom in the rigid cage. The importance of the relativistic effects indicates that the excellent agreement of the NR DFT results of Ref. [39] with the experiment is accidental.

In 2008, we have calculated the ^{129}Xe NMR CS in Xe@C_{60} using the DFT calibrated against accurate CCSD(T) calculations, including the relativistic contributions, corrections for intramolecular dynamics, and implicit solvent effects. However, a large discrepancy between the calculated (152.9 ppm)[52] and experimental (179.2 ppm)[51] isotropic ^{129}Xe shift was obtained. This was attributed to the missing description of explicit solvent and its dynamics in the calculations.

The aim of our present work is to include explicit solvent in the calculations to faithfully simulate the experimental conditions and to investigate the role of different physical contributions to the ^{129}Xe NMR CS for the Xe@C_{60} dissolved in liquid benzene. Ultimately, we aim at development of the computational protocol to calculate the ^{129}Xe NMR CSs in Xe atom guest–host systems, with inclusion of relativistic, solvent, and dynamic contributions to the ^{129}Xe shift, thus modeling the experimental conditions.

Recently, we have also built a computational protocol for calculating the ^{129}Xe CS of Xe atom dissolved in liquids.[53] The dynamically averaged isotropic ^{129}Xe shift for Xe atom dissolved in benzene at 300 K was calculated to be 191.4 $\pm$ 2.5 ppm, reaching the excellent agreement with previously reported experimental data ranging from 188 to 195 ppm.[51,54,55]

The models used in Refs. [52,53] are connected in this article to study the Xe@C_{60} molecule dissolved in liquid benzene. In our model, we calculate the ^{129}Xe shift quantum chemically (QC) and evaluate the dynamic and solvent effects by averaging the QC calculations of snapshots from molecular dynamics (MD) trajectory of the system.[53] The relativistic corrections to the ^{129}Xe nuclear magnetic shielding are evaluated at the Breit–Pauli perturbation theory (BPPT) level.[56–58] In this way, the computational protocol provides dynamically averaged relativistic ^{129}Xe CS in Xe@C_{60} with effects of cage dynamics, and effects of explicit dynamical solvent included in the calculations. Due to the piecewise approximation used, the roles and relative size of different physical contributions can be assessed.

Methods

Molecular dynamics simulations

The AMBER 11 software[59] was used in MD simulations. The MD simulation protocol and the general Amber force field[60] parameters for the Xe atom and benzene molecule have been adopted from previously developed model for simulation of Xe atom dissolved in benzene,[53] see Supplementary Information, Table S1. Bonds involving hydrogen atoms were constrained using the SHAKE algorithm.[61]

Although all carbons in C_{60} are naturally equivalent, for technical reasons, they had to be defined in a force field as five different atom types (see Supplementary Information, Figs. S1–S5). To define the C_{60} molecule using these atom types, new force field parameters were developed. The parameters were based on the optimized geometry and calculated frequencies performed at the DFT BP86/def-TZVP[62–64] level in the Turbomole 6.0 package.[65] Reliability of this level of theory for Xe@C_{60} geometry was already shown in Ref. [52]. The force field parameters were found by the linear least-square fitting technique, where the optimized function was sum of squares of differences between QM and molecular mechanics (MM) frequencies.

In simulations with explicit solvent, the equilibrated solvent box was used to solvate the Xe@C_{60} system with a buffer set to 25 Å. This provided a rectangular solvent box with the edge of size 63.5 Å and 1204 molecules of solvent. The cubic box was built and minimized using the periodic boundary conditions. In the first equilibration step, the system was heated for 200 ps from 1 to 298 K within the constant volume and temperature (NVT) condition applying the Langevin stochastic thermostat. The second equilibration step was 500 ps of MD simulation using the constant pressure and temperature (NPT) ensemble at 1 atm (Supplementary Information, Fig. S1). The final size of the box edge after equilibration was 56.6 Å.

The production run was taken for 5 ns at NPT conditions. For refining the distribution functions, additional 5 ns NPT trajectory was performed. Similarly, in the MD simulation of Xe@C_{60} without solvent box, Xe@C_{60}(*g*), the system was heated for 200 ps from 1 to 298 K and following 10 ns production run was performed. Two hundred snapshots (each 25 ps) of the production run were used in calculations of the ^{129}Xe shielding constant.

All simulations were done using integration time step of 1 fs and coordinates were stored each 0.5 ps. The subsequent

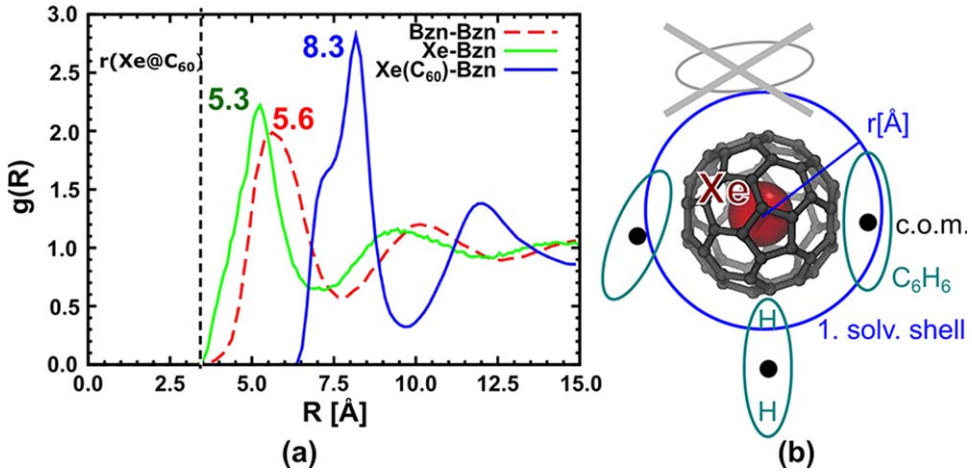

Figure 2. a) Radial distribution functions for different MD simulations (using distance between Xe atom and center of mass of benzene molecule). Bzn-Bzn and Xe-Bzn curves were taken from Ref. [53]. The vertical line corresponds to the mean radius of Xe@C_{60}. b) Scheme of the truncation of the snapshots beyond the first solvation shell for use in the QM calculations. The circle represents the radius of the first solvation shell taken from the RDF shown in (a).

DFT nuclear magnetic shielding calculations used snapshots truncated to the first solvation shell (Fig. 2), that is, the solvent molecules beyond the first solvation shell were removed from the snapshot unless otherwise mentioned. The relevance of such approximation was assessed in Ref. [53].

Nonrelativistic calculations of ^{129}Xe NMR CS

Nuclear magnetic shielding calculations were performed at the DFT level of theory using the Gauge-Independent Atomic Orbital approximation.[66,67] as implemented in the Gaussian 09 software, Ref. [68]. Based on the previous calibration of the density functional methods against accurate CCSD(T) for nonrelativistic ^{129}Xe CS,[52] the exchange–correlation BHandHLYP[62,69,70] functional was used in combination with [22s17p14d2f/15s13p11d2f] basis set for Xe (referred to as MHA[52]) and the split-valence polarization (SVP) [71] basis set for C and H atoms.

For testing purposes, the implicit solvent was simulated by the polarizable continuum model (PCM),[72,73] using the integral equation formalism variant of PCM, IEF-PCM method[74] implemented in Gaussian 09. Number of snapshots used in the production run was chosen based on the calculated cumulative average check showing the evolution of the averaged value for nonrelativistic CS of the Xe@C_{60} in solvent (Supplementary Information, Figure S2).

It is important to mention that nonrelativistic calculations of nuclear magnetic shielding were found to be rather sensitive to the accuracy of the DFT numerical integration grid, see Supplementary Information, Tables S2–S4. Hence, more accurate "ultrafine" grid as defined in the Gaussian 09 code was used in the production work.

Relativistic Breit–Pauli perturbation theory calculations

For details of BPPT, we refer to original papers.[56–58] Relativistic BPPT corrections were calculated using the Dalton 2011[75] package. The common gauge origin was placed at the nucleus of the Xe atom. The same DFT functional, BHandHLYP,[62,69,70] as for nonrelativistic contribution was used in calculations. It was shown previously[52,53] that typically only five (BPPT-5) and, in case of Xe dissolved in benzene, only three (BPPT-3) BPPT terms of total of 16 are responsible for over 95% of the full-BPPT relativistic correction to the isotropic ^{129}Xe CS. In the production work, only the three most important BPPT contributions (BPPT-3) were taken into account in the dynamical averaging calculations, because the inclusion of other terms was not affordable for our extended system. These were the second-order singlet $\sigma^{p\text{-}KE/OZ}$ and the third-order singlet $\sigma^{p/mv}$ and $\sigma^{p/Dar}$ terms. All the 16 BPPT contributions were evaluated only for the MM-minimized single-point geometry of Xe@C_{60} to check the limitations of the BPPT-3 in the present model.

Uncontracted FIVu61 basis set [27s23p22d2f] developed by Lantto and Vaara[31] was used for Xe and the SVP basis set[71] was used for C and H. The initial guess in the SCF step was precalculated using the Turbomole 6.0 software. As the BPPT method is computationally demanding, the effect of solvent on the BPPT contribution was assessed by calculations of snapshots with the solvation shell reduced to the closest 20 benzene molecules. Reliability of this approach is checked in section Results and Discussion.

Other details

The nuclear shielding constant was converted into NMR CS according to

$$\delta = (\sigma_{ref} - \sigma)/(1 - \sigma_{ref}) \quad (1)$$

σ and σ_{ref} are the calculated shielding constants of Xe in the environment in question and in the reference system, respectively. For practical reasons, the corresponding reference system was bare Xe atom, calculated at the same level of theory. This presents only small error when comparing the computational results to the experimental ones using Xe gas as a reference.

Results and Discussion

MD simulations of the Xe@C_{60} in benzene: structural aspects

To study the role of individual effects contributing to the ^{129}Xe NMR CS in Xe@C_{60} system, three different MD

Table 1. Radius of gyration of the C_{60} cage ($\sim C_{60}$ mean radius) R and RMSD calculated from the 1ns (2000 frames) MD trajectory at 298 K and 1 atm.

MD run	R (Å)	RMSD (Å)
$C_{60}(g)$	3.556	8.34×10^{-3}
$Xe@C_{60}(g)$	3.573	8.09×10^{-3}
$Xe@C_{60}$(Bzn)	3.570	8.19×10^{-3}

simulations were performed. The first model contained only the C_{60} fullerene molecule. In the second model, Xe atom was placed inside the C_{60} system leading to the gas-phase $Xe@C_{60}(g)$. In the third model, the $Xe@C_{60}$ was embedded in a box of benzene molecules. Mean radius of the C_{60} cage and root-mean-square deviation (RMSD) values for these three situations are summarized in Table 1. Interestingly, the sum of van der Waals radii of C and Xe atoms (1.908 + 2.231 = 4.139 Å) is markedly larger than the mean radius of 3.556 Å calculated for C_{60} (Table 1); the Xe atom thus appears compressed in $Xe@C_{60}$. However, due to attractive dispersion forces, the interaction energy for Xe in C_{60} is negative, it was calculated as −84.0 kJ mol^{-1} at the spin-component scaled 2nd-order perturbation theory (SCS-MP2) level.[76]

The diameter of the C_{60} cage is larger for $Xe@C_{60}(g)$ as compared to that of empty $C_{60}(g)$ cage (3.573 vs. 3.556 Å), and the cage of $Xe@C_{60}(g)$ is more rigid (compare RMSD values in Table 1). The solute–solvent interactions in $Xe@C_{60}$(Bzn) reduce the diameter of the cage rather marginally (to 3.570 Å) but somewhat increase the flexibility of the cage.

The shape of Xe–Bzn radial distribution function for the $Xe@C_{60}$(Bzn), using center of mass of a benzene molecule for Xe-Bzn distance in Figure 2 is similar to that for free Xe atom dissolved in benzene (studied in Ref. [53]). The peaks for $Xe@C_{60}$(Bzn) are shifted toward larger values as compared to Xe atom dissolved in the benzene[53] (e.g., 5.3 vs. 8.3 Å for the first solvation shell) reflecting the difference between the smaller Xe atom and the larger $Xe@C_{60}$ system.

Snapshots for QM calculations were constructed by reducing the full snapshots of the simulation box to retain only the $Xe@C_{60}$ and the first solvation shell, as indicated in Figure 2b.[53] More details about this procedure and justification of using the first solvent shell approximation can be found in Ref. [53].

Effect of dynamics and solvent on nonrelativistic ^{129}Xe NMR CS, δ_{NR}

To calculate the averaged NR isotropic ^{129}Xe NMR CS, δ_{NR}, 200 individual MD snapshots of the 5 ns trajectory (25ps step) with solvent box reduced to the first solvation shell (Fig. 2b) were used. The fluctuations of the calculated δ_{NR} as well as the normal distribution of the calculated values are illustrated in Figure 3.

The $Xe@C_{60}$ structure was also minimized using MM, with the same parameters as used for the MD simulations, and the ^{129}Xe shift was calculated. This allowed us to separate individual effects of the cage dynamics and solvent reflected in the final δ_{NR}, see Table 2. Comparing the ^{129}Xe shift in MM--optimized structure (δ_{NR} = 132.1 ppm) with the averaged value from the MD simulation of $Xe@C_{60}(g)$ (δ_{NR} = 145.1 ppm) gives the pure effect of the cage and Xe atom dynamics of 13 ppm. Furthermore, by comparing the result for $Xe@C_{60}(g)$ with that for the $Xe@C_{60}$(Bzn) simulation in solvent but removing the solvent box in the shielding constant calculations (δ_{NR} = 144.3 ppm), an indirect effect of the modulation of the $Xe@C_{60}$ structure by dynamical solvent on the ^{129}Xe shift is obtained. This effect is rather small and deshielding, −0.8 ppm. Including the benzene solvent molecules of the first solvation shell resulted in the averaged final value of 156.3 ppm for δ_{NR}. Thus, the electronic effect of the explicit dynamical solvent represents 12 ppm and the total effect of the dynamical solvent gives 11.2 ppm. The collective dynamic motions of the cage and solvent represent overall contribution of +24.2 ppm to δ_{NR}.

The standard deviations of δ_{NR} in Table 2 indicate how the instantaneous values of ^{129}Xe shift are dispersed from the mean value. They mimic the fluctuations of the electronic structure around the Xe atom during the MD simulations. The values for σ_x in Table 2 ranging from 7.1 to 8.3 ppm for $Xe@C_{60}$ are much smaller than σ_x = 54.4 ppm calculated for

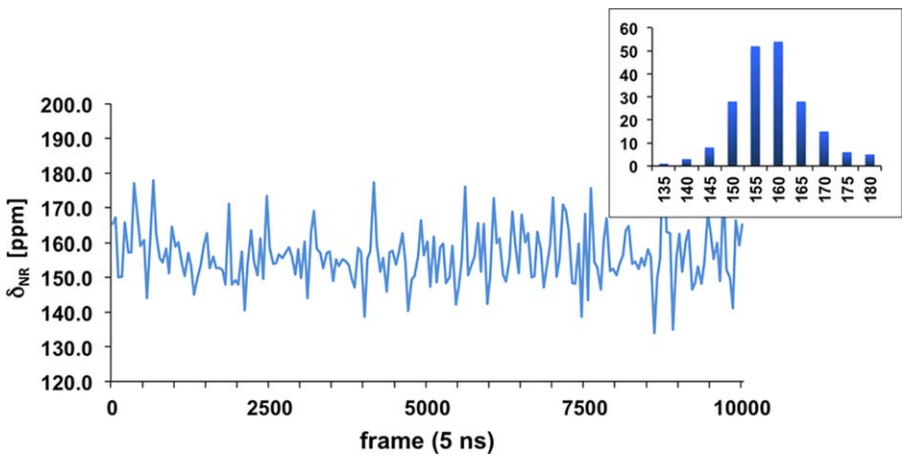

Figure 3. Time evolution of the calculated (BHandHLYP/MHA/SVP) nonrelativistic ^{129}Xe chemical shift, δ_{NR}, using 200 equidistant snapshots of the 5 ns trajectory obtained from the MD simulation of $Xe@C_{60}$(Bzn). The inset shows normal distribution of δ_{NR}. [Color figure can be viewed in the online issue, which is available at wileyonlinelibrary.com]

Table 2. BHandHLYP/SVP/MHA calculated nonrelativistic ^{129}Xe chemical shift, δ_{NR}, using 200 snapshots of the 5ns trajectory.

	MM Xe@C_{60}	MD Xe@C_{60}(*g*)	MD Xe@C_{60}[a]	MD Xe@C_{60}(Bzn)
δ(ppm)	132.1	145.1 (7.1)	144.3 (7.4)	156.3 (8.3)

Standard deviations, σ_x, in parentheses.[a]Using snapshots from Xe@C_{60}(Bzn) simulation but removing all benzenes in the nuclear shielding constant calculations.

the Xe atom in benzene, Ref. [53]. Apparently, the Xe atom in the C_{60} cage is well screened from the fluctuating environment of the benzene solvent.

To check the applicability of implicit solvent model, a simple test was performed. A subset of 21 snapshots from the Xe@C_{60}(Bzn) trajectory was selected, the benzene molecules were removed, and ^{129}Xe nuclear magnetic shielding was calculated for each snapshot with and without the PCM model on. The values using PCM show only marginal differences from those for the gas-phase system but large differences from those with benzene molecules included (Supplementary Information, Table S5). Thus, the solvent must be considered explicitly in the simulations of Xe@C_{60}; PCM approximation fails here to describe correctly the solvent effects. This is not a general case, though. Many examples can be found in the literature, where the simulation of solvent effects using implicit solvent models is sufficient. [77–79] There are also situations, where PCM gives better results than explicit dynamical solvent,[80] due to inaccurate force fields in MD.

Relativistic BPPT contribution to ^{129}Xe NMR CS, δ_{BPPT}

Total dynamically averaged nonrelativistic ^{129}Xe CS of 156.3 ppm calculated in previous section still deviates significantly from the experimental value of 179.2 ppm. Hence, we now proceed to the evaluation of the relativistic corrections, δ_{BPPT}.

The relativistic BPPT calculations are an order of magnitude more computationally demanding than the nonrelativistic calculations. Thus, the full BPPT was only affordable for a single-point calculation. BPPT-3 approximation[53] (see Methods) was used in the snapshot calculations, using only limited subset of snapshots—21 in the present case. Furthermore, it was not affordable to include the complete first solvation shell in the dynamical averaging calculations. Hence, we checked if the approximation of the first solvent shell could be still reduced. We selected three MD frames that showed extreme values of ^{129}Xe shift in the nonrelativistic calculations—one with the lowest ^{129}Xe shift, one with the highest one, and one with the value close to the average. Subsequently, we preserved 0, 5, 10, 15, and 20 benzene molecules (at the NR level up to full size) of the first solvation shell in the calculations and followed the convergence of both δ_{NR} and δ_{BPPT-3} in Figure 4 (more details are given in Supplementary Information, Tables S6 and S7).

Convergence of the δ_{NR} values evident from Figure 4a indicates that the inclusion of 20 closest solvent molecules should be sufficient for producing the results deviating by less than 1 ppm from those obtained using the full first solvation shell approximation (see Table 3). Now, using the MM-minimized Xe@C_{60} structure we obtain static relativistic BPPT-3 contribution to the ^{129}Xe shift of +11.2 ppm (Table 3). The dynamically-averaged BPPT-3 contribution, estimated from an average over 21 snapshots of the MD Xe@C_{60}(*g*) simulation is by 1.1 ppm larger (+12.3 ppm) than the static value (Table 3). The effect of dynamical solvent is estimated to additional ~+1 ppm from Figure 4. The indirect effect of solvent on the ^{129}Xe shift via changes in Xe@C_{60} structure is negligible (−0.1 ppm, Table 3). This gives the estimate of dynamically-averaged

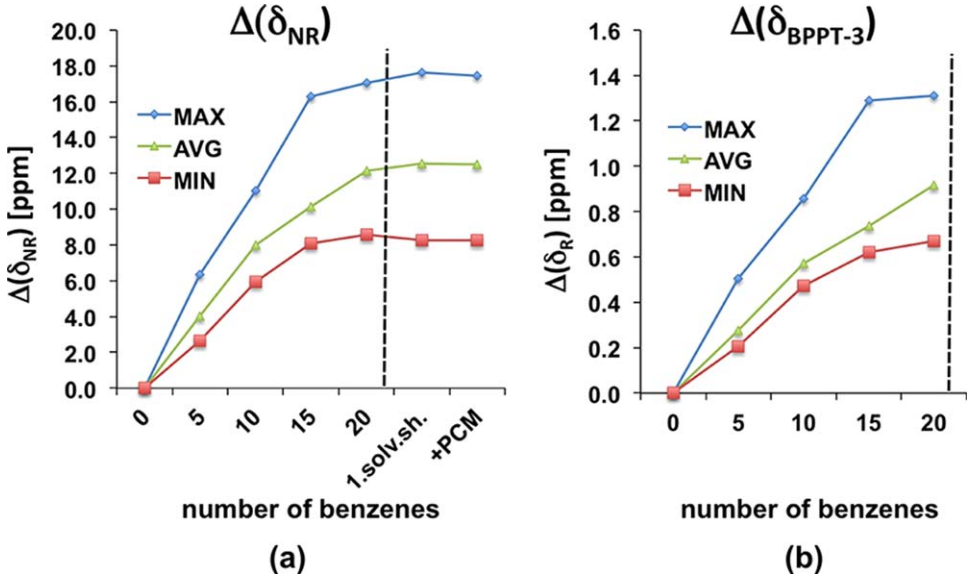

Figure 4. Calibration of the solvent model using selected snapshots. AVG is snapshot with the ^{129}Xe shift closest to the averaged nonrelativistic chemical shift. MIN/MAX corresponds to snapshots with the lowest/highest value of ^{129}Xe shift. $\Delta(\delta_{NR/R})$ – changes of ^{129}Xe shift (ppm) in Xe@C_{60} with respect to number of closest benzene molecules included in the calculations. [Color figure can be viewed in the online issue, which is available at wileyonlinelibrary.com]

Table 3. Relativistic BPPT-3 contributions, δ_{BPPT-3} to the ^{129}Xe chemical shift (in ppm).

	p-KE/OZ	p/mv	p/Dar	δ_{BPPT-3}
MM, Xe@C_{60}	−20.4	39.6	−7.9	11.2
MD, Xe@C_{60}(*g*)	−22.2	43.7	−9.1	12.3
MD, Xe@C_{60}[a]	−22.4	44.1	−9.2	12.4
MD, Xe@C_{60}(Bzn)[b]				∼13.4

Using a subset of 21 snapshots of 5 ns trajectory. [a] Using snapshots from Xe@C_{60}(Bzn) simulation but removing all benzenes in the shielding calculations. [b] Including only 20 closest solvent molecules.

relativistic BPPT-3 contribution to ^{129}Xe NMR CS of ∼13.4 ppm. Notice, that impact of the dynamic and solvent effects on the relativistic BPPT-3 contribution to the ^{129}Xe CS is proportionally of the same magnitude as obtained at the nonrelativistic level, 16 and 15%, respectively.

A single-point full BPPT calculation was affordable to test the reliability of BPPT-3 approximation. Additional shift of ∼3 ppm was obtained (Table 4). A more detailed aspect in Table 4 reveals that the main difference between the full BPPT and BPPT-3 originates from the spin-orbit (SO) induced Fermi-contact (FC) and spin-dipolar (SD) terms. Interestingly, the FC and SD terms were found rather small in the system of Xe atom dissolved in liquid,[53] while they were found rather large in xenon molecules.[30,34] It has been aforementioned that Xe atom appears somewhat compressed in Xe@C_{60}. It can be speculated that the SO-induced BPPT contributions become more important at shorter distances between Xe and surrounding atoms. Thus, for strongly confined Xe atom guest–host systems, either full BPPT or at least BPPT-5 approximations should be used instead

Table 4. Calculated BPPT contributions to ^{129}Xe chemical shift in Xe@C_{60}.[a]

BPPT term[b]	σ(Xe)	σ(Xe@C_{60}, MM)	δ
con	−660.5	−660.5	0.0
dip	0.0	0.0	0.0
d-ke	−557.2	−557.5	0.3
p-OZ	−41.5	−41.7	0.2
d/mv	945.4	945.4	0.0
d/Dar	−503.7	−503.7	0.0
p/OZ-KE	152.6	152.6	−0.1
p-KE/OZ	0.0	20.4	−20.4
FC/SZ-KE	2049.5	2049.4	0.1
SD/SZ-KE	0.0	0.0	0.0
FC-II(1)	−350.4	−350.3	−0.1
SD-II(1)	69.4	69.4	0.0
p/mv	0.0	−39.6	39.6
p/Dar	0.0	7.9	−7.9
FC-I(1)	0.0	−0.7	0.7
FC-I(2)	0.0	−0.5	0.5
SD-I(1)	0.0	−1.1	1.1
SD-I(2)	0.0	−0.3	0.3
BPPT-3			11.2
BPPT-5			13.7
$BPPT_{total}$			14.2

In ppm. [a] At BHandHLYP/MHA/SVP level. MM-optimized structure used. [b] For the theoretical basis and interpretation of the different terms, see Ref. [56].

BPPT-3. However, it was not affordable to run more BPPT-5 calculations in our case.

The overall dynamically averaged BPPT relativistic contribution, δ_{BPPT} = 16.4 ppm represents ∼9% in the total calculated ^{129}Xe CS, 172.7 ppm. This result is close to the previously reported dynamically averaged relativistic ^{129}Xe CS contribution (∼8%) for Xe atom dissolved in benzene.[53]

Summing up individual contributions to the ^{129}Xe NMR CS: general comments

The total calculated ^{129}Xe NMR CS in Xe@C_{60} dissolved in benzene after inclusion of relativistic, dynamic, and solvent effects is +172.7 ppm, which deviates by 6.5 ppm from the experimental value of 179.2 ppm.[51] The individual physical contributions are schematically shown in Figure 5. The main portion of the total ^{129}Xe shift of 132.1 ppm is obtained from the nonrelativistic calculations of the Xe@C_{60} molecule *in vacuo* at rest. The nonrelativistic contribution originating in dynamics of the cage and dynamical solvent represents additional 24.2 ppm, of which nearly one half, 13 ppm is estimated to be due to molecular motions of the Xe@C_{60} system and approximately 11.2 ppm originates in the effects of the dynamical solvent. The total relativistic effect, obtained by the Breit–Pauli perturbation theory approximation, amounts to 16.4 ppm, of which 14.2 ppm arises from the full-BPPT calculation of the static Xe@C_{60} molecule at rest *in vacuo*, and 2.2 ppm arises from the estimated dynamic and solvent effects on the relativistic BPPT contribution.

From another point of view, summing up the NR and relativistic BPPT contributions, we obtain 146.3 ppm (85%) for static gas-phase Xe@C_{60} molecule, 14.1 ppm (8%) for the effect of the dynamical cage, and 12.3 ppm (7%) for the effect of the dynamical solvent. The large effect of dynamical solvent nicely illustrates the high sensitivity of the ^{129}Xe shift. Although the Xe atom is encapsulated in C_{60}, the solvent environment gives rise to measurable changes in the ^{129}Xe shift, even when using Xe atom dissolved in the solvent as a reference. This is also evident from the experimental difference between the ^{129}Xe shift in Xe@C_{60} dissolved in benzene (179.2) and Xe atom dissolved in benzene (188.1) ppm.[51]

It is reasonable to assume that the remaining discrepancy between the calculated and experimental value of 6.5 ppm arises from the cumulated errors in the piecewise approximation employed. The possible inaccuracies arise from various sources: MD potential, employed DFT functional, approximation of using the first solvent shell only (<2 ppm, Ref. [53]), missing solvent and dynamic corrections to the full-BPPT approximation (<1 ppm), errors due to the BPPT approximation itself (not easy to assess for the present system), errors due to basis sets used, and errors from statistical averaging (estimated here by blocking method[53] to ±0.6 ppm). The basis set superposition error estimated from selected snapshots would further deteriorate the calculated results by approximately −0.5 ppm (Supplementary Information, Table S8**)**. The discrepancy of another ∼−0.5 ppm caused by using Xe atom as reference instead of Xe gas should be mentioned

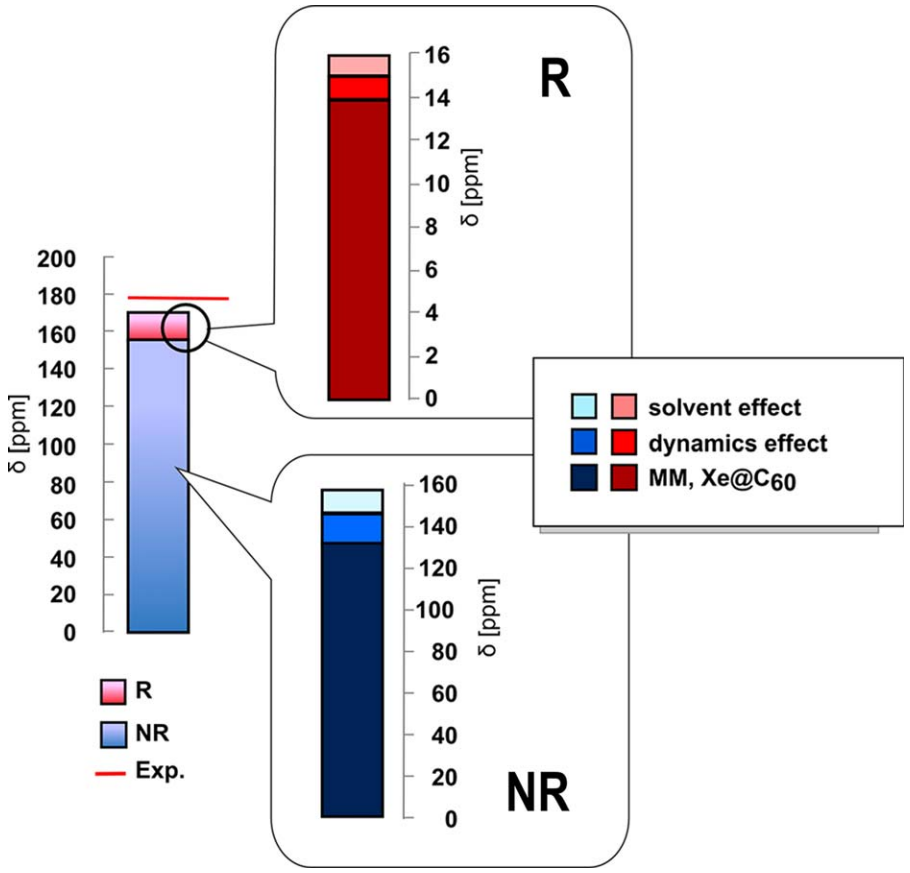

Figure 5. Individual contributions to the total calculated ^{129}Xe NMR chemical shift in Xe@C_{60} dissolved in benzene. NR – the nonrelativistic ^{129}Xe shift, R – BPPT relativistic contribution to the ^{129}Xe shift.

here.[43,51] In fact, the temperature of the measurement was not specified in the experimental paper.[51] None of these possible errors is expected to be larger than 1–2 ppm but the cumulative effect could be responsible for the remaining difference of 6.5 ppm between the theory and the experiment.

From this and previous studies[52,53] is clear that relativistic corrections present typically about 8–9% of the total calculated isotropic ^{129}Xe NMR CS. For assessment of the relativistic effects, BPPT-3 approximation will do well in case of weakly bonded ^{129}Xe atom, whereas at least BPPT-5 has to be used for strongly confined or chemically bound Xe atom situation. Furthermore, the dynamic and solvent effects appear to have similar proportional effect on the nonrelativistically calculated ^{129}Xe CS as on the relativistic BPPT corrections to it. Hence, relativistic corrections can be simply estimated in more complicated studies.

Summarizing, despite the abovementioned inaccuracies, the piecewise approximation presented here provides a detailed insight and serves as a good starting point in the future simulations of confined Xe guest–host systems.

Conclusions

The isotropic ^{129}Xe NMR CS for Xe@C_{60} dissolved in benzene was calculated by combining classical MD and QC calculations using nonrelativistic DFT as well as relativistic Breit–Pauli perturbation theory at the DFT level. Systematic piecewise approximation was applied to identify the dynamic and solvent contributions to the total ^{129}Xe NMR CS both at the nonrelativistic and relativistic BPPT levels. The dynamic contribution of Xe@C_{60} cage represents about 8% (δ_{NR} ~13 ppm, $\delta_{BPPT-3} \sim 1$ ppm) of the total value and the modulation of electronic contribution by the solvent 7% ($\delta_{NR} \sim 11.2$ ppm, $\delta_{BPPT-3} \sim 1$ ppm) of the total calculated ^{129}Xe NMR CS. The dynamically-averaged solvent-included relativistic correction represents about 9% (16.4 ppm) of the total calculated ^{129}Xe CS. The final calculated value of 172.7 ppm is in a reasonable agreement with the experimental CS of 179.2 ppm, reflecting the limitations of the computational model.

The developed approach serves as a prototypical model for the ^{129}Xe NMR calculations of Xe atom guest–host systems. Particularly interesting for future directions appear the simulations and understanding of the ^{129}Xe NMR parameters in ^{129}Xe NMR biosensors, such as cryptophanes, with potential impact in MRI and medicine.

Acknowledgments

The authors thank to Perttu Lantto and Juha Vaara for the BPPT version of the Dalton code. Computational resources were provided by the MetaCentrum under the program LM2010005 and the CERIT-SC

under the program Centre CERIT Scientific Cloud, part of the Operational Program Research and Development for Innovations, Reg. no. CZ.1.05/3.2.00/08.0144.

Keywords: ^{129}Xe NMR · Xe@C_{60} · dynamical averaging · explicit solvent · relativistic effects

How to cite this article: S. Standara, P. Kulhánek, R. Marek, M. Straka, *J. Comput. Chem.* **2013**, *00*, 000–000. DOI: 10.1002/jcc.23334

[1] M Gerken, G. Schröbilgen, *Coord. Chem. Rev.* **2000**, *197*, 335.
[2] C. I. Ratcliffe, *Annu. Rep. NMR Spectrosc.* **1998**, *36*, 123.
[3] J. Jokisaari, In NMR of Ordered Liquids; E. E. Burnell, C. A. de Lange, Eds; Kluwer, Dordrecht, Singapore, **2003**; pp. 109–135.
[4] J. Jokisaari, In Nuclear Magnetic Resonance Spectroscopy of Liquid Crystals; R. Dong, Eds; World Scientific Publishing Co Pte Ltd, Dordrecht, Singapore, **2009**; pp. 79–116.
[5] J. Jokisaari, *Prog. Nucl. Magn. Reson. Spectr.* **1994**, *26*, 1.
[6] M. P. Ledbetter, G. Saielli, A. Bagno, N. Tran, M. V. Romalis, *Proc. Natl. Acad. Sci. USA* **2012**, *109*, 12393.
[7] D. Raftery, B. F. Chmelka, In *NMR Basic Principles and Progress*, Vol. *30*; **1994**, p. 111, Springer, Heidelberg.
[8] K. V. Romanenko, *Annu. Rep. NMR Spectrosc.* **2010**, *69*, 1.
[9] Y. P. Yampolskii, *Russ. Chem. Rev.* **2007**, *76*, 59.
[10] B. Nagasaka, H. Omi, T. Eguchi, H. Nakayama, N. Nakamura, *Chem. Phys. Lett.* **2001**, *340*, 473.
[11] L. Yang, C. Tulk, D. Klug, I. L. Moudrakovski, C. I. Ratcliffe, J. A. Ripmeester, B. Chakoumakos, L. Ehm, D. Martin, J. Parise, *Proc. Nat. Acad. Sci.* **2009**, *106*, 6060.
[12] J. A. Ripmeester, J. S. Tse, C. I. Ratcliffe, B. M. Powell, *Nature* **1987**, *325*, 135.
[13] I. L. Moudrakovski, A. Sanchez, C. I. Ratcliffe, J. A. Ripmeester, *J. Phys. Chem. B* **2000**, *104*, 7306.
[14] M. A. Springuel-Huet, A. Nossov, A. Adem, F. Guenneau, C. Volkringer, T. Loiseau, G. Ferey, A. Gedeon, *J. Am. Chem. Soc.* **2010**, *132*, 11599.
[15] K. J. Ooms, R. E. Wasylishen, *Microporous Mesoporous Mater.* **2007**, *103*, 341.
[16] A. Comotti, S. Bracco, L. Ferretti, M. Mauri, R. Simonutti, P. Sozzani, *Chem. Commun.* **2007**, *2007*, 350.
[17] O. Taratula, I. J. Dmochowski, *Curr. Op. Chem. Bio.* **2010**, *14*, 97.
[18] P. Berthault, G. Huber, H. Desvaux, *Prog. Nucl. Magn. Reson. Spec.* **2009**, *55*, 35.
[19] M. J. Chambers, P. A. Hill, J. A. Aaron, Z. Han, D. W. Christianson, N. N. Kuzma, I. J. Dmochowski, *J. Am. Chem. Soc.* **2009**, *131*, 563.
[20] A. Schlundt, W. Kilian, M. Beyermann, M. Sticht, S. Günther, S. Höpner, K. Falk, O. Roetzschke, L. Mitschang, C. Freund, *Angew. Chem. Int. Ed.* **2009**, *48*, 4142.
[21] D. R. Jacobson, N. S. Khan, R. Collé, R. Fitzgeral, L. Laureano-Pérez, Y. Bai, I. J. Dmochowski, *Proc. Natl. Acad. Sci. USA* **2011**, *108*, 0969.
[22] K. F. Stupic, Z. I. Cleveland, G. E. Pavlovskaya, T. Meersmann, *J. Magn. Reson.* **2011**, *208*, 58
[23] G. K. Seward, Y. Bai, N. S. Khan, I. J. Dmochowski, *Chem. Sci.* **2011**, *2*, 1103.
[24] F. Schilling, L. Schröder, K. K. Palaniappan, S. Zapf, D. E. Wemmer, A. Pines, *Chem. Phys. Chem.* **2010**, *11*, 3529.
[25] L. Schröder, *Phys Med.* **2013**, *29*, 3.
[26] J. Sloniec, M. Schnurr, C. Witte, U. Resch-Genger, L. Schröder, A. Hennig, *Chem. Eur. J.* **2013**, *19*, 3110.
[27] C. Boutin, A. Stopin, F. Lenda, T. Brotin, J.-P. Dutasta, N. Jamin, A. Sanson, Y. Boulard, F. Leteurtre, G. Huber, A. Bogaert-Buchmann, N. Tassali, H. Desvaux, M. Carrière, P. Berthault, *Bioorg. Med. Chem.* **2011**, *19*, 4135.
[28] P. Berthault, A. Bogaert-Buchmann, H. Desvaux, G. Huber, Y. Boulard, *J. Am. Chem. Soc.* **2008**, *130*, 16456.
[29] L. Schröder, T. J. Lowery, C. Hilty, D. E. Wemmer, A. Pines, *Science* **2006**, *314*, 446.
[30] M. Straka, P. Lantto, M. Räsänen, J. Vaara, *J. Chem. Phys.* **2007**, *127*, 234314.
[31] P. Lantto, J. Vaara, *J. Chem. Phys.* **2007**, *127*, 084312.
[32] J. Cukras, J. Sadlej, *Chem. Phys. Lett.* **2008**, *467*, 18.
[33] A. Bagno, G. Saielli, *Chem. Eur. J.* **2003**, *9*, 1486.
[34] P. Lantto, S. Standara, S. Riedel, J. Vaara, M. Straka, *Phys. Chem. Chem. Phys.* **2012**, *14*, 10944.
[35] J. Cukras, J. Sadlej, *Phys. Chem. Chem. Phys.* **2011**, *13*, 15455.
[36] J. H. Kantola, J. Vaara, T. Rantala, J. Jokisaari, *J. Chem. Phys.* **1997**, *107*, 6470.
[37] J. Autschbach, E. Zurek, *J. Phys. Chem. A* **2003**, *107*, 4967.
[38] M. Bühl, S. Patchkovskii, W. Thiel, *Chem. Phys. Lett.* **1997**, *275*, 14.
[39] D. N. Sears, C. J. Jameson, *J. Chem. Phys.* **2003**, *118*, 9987.
[40] J. Lintuvuori, M. Straka, J. Vaara, *Phys. Rev. E* **2007**, *75*, 31707.
[41] C. J. Jameson, D. N. Sears, A. C. de Dios, *J. Chem. Phys.* **2003**, *118*, 2575.
[42] D. N. Sears, R. E. Wasylishen, T. Ueda, *J. Phys. Chem. B* **2006**, *110*, 11120.
[43] C. J. Jameson, D. N. Sears, S. Murad, *J. Chem. Phys.* **2004**, *121*, 9581.
[44] C. J. Jameson, D. Stueber, *J. Chem. Phys.* **2004**, *120*, 10200.
[45] D. Stueber, C. J. Jameson, *J. Chem. Phys.* **2004**, *120*, 1560.
[46] D. N. Sears, C. J. Jameson, *J. Chem. Phys.* **2003**, *119*, 12231.
[47] M. Hanni, P. Lantto, M. Iliaš, H. J. Aa. Jensen, J. Vaara, *J. Chem. Phys.* **2007**, *127*, 164313.
[48] M. Hanni, P. Lantto, N. Runeberg, J. Jokisaari, J. Vaara, *J. Chem. Phys.* **2004**, *121*, 5908.
[49] M. Hanni, P. Lantto, J. Vaara, *Phys. Chem. Chem. Phys.* **2009**, *11*, 2485.
[50] A. Bagno, G. Saielli, *Chem. Eur. J.* **2012**, *18*, 7341.
[51] M. S. Syamala, R. J. Cross, M. Saunders, *J. Am. Chem. Soc.* **2002**, *124*, 6216.
[52] M. Straka, P. Lantto, J. Vaara, *J. Phys. Chem. A* **2008**, *112*, 2658.
[53] S. Standara, P. Kulhánek, P. Bouř, R. Marek, J. Horníček, M. Straka, *Theor. Chem. Acc.* **2011**, *129*, 677
[54] T. R. Stengle, N. V. Reo, K. L. Williamson, *J. Phys. Chem.* **1981**, *85*, 3772.
[55] K. W. Miller, N. V. Reo, A. J. M. S. Uiterkamp, D. P. Stengle, T. R. Stengle, K. L. Williamson, *Proc. Natl. Acad. Sci. USA* **1981**, *78*, 4946.
[56] J. Vaara, P. Manninen, P. Lantto, In Calculations of NMR and EPR Parameters: Theory and Applications; M. Kaupp, M. Bühl, V. G. Malkin, Eds; Wiley-VCH, Weinheim, **2004**; pp. 209–226.
[57] P. Manninen, P. Lantto, J. Vaara, K. Ruud, *J. Chem. Phys.* **2003**, *119*, 2623.
[58] (a) P. Manninen, K. Ruud, P. Lantto, J. Vaara, *J. Chem. Phys.* **2005**, *122*, 114107; (b) Erratum: *J. Chem. Phys.* **2006**, *124*, 149901.
[59] D. A. Case, T. A. Darden, T. E. Cheatham, III, C. L. Simmerling, J. Wang, R. E. Duke, R. Luo, R. C. Walker, W. Zhang, K. M. Merz, B. Roberts, B. Wang, S. Hayik, A. Roitberg, G. Seabra, I. Kolossváry, K. F. Wong, F. Paesani, J. Vanicek, J. Liu, X. Wu, S. R. Brozell, T. Steinbrecher, H. Gohlke, Q. Cai, X. Ye, J. Wang, M. J. Hsieh, G. Cui, D. R. Roe, D. H. Mathews, M. G. Seetin, C. Sagui, V. Babin, T. Luchko, S. Gusarov, A. Kovalenko, P. A. Kollman, AMBER 11, University of California: San Francisco, **2010**.
[60] J. M. Wang, R. M. Wolf, J. W. Caldwell, P. A. Kollman, D. A. Case, *J. Comput. Chem.* **2004**, *25*, 1157.
[61] J. P. Ryckaert, G. Ciccotti, H. J. C. Berendsen, *J. Comput. Phys.* **1977**, *23*, 327.
[62] A. D. Becke, *Phys. Rev. A* **1988**, *38*, 3098.
[63] J. P. Perdew, *Phys. Rev. B* **1986**, *33*, 8822.
[64] F. Weigend, R. Ahlrichs, *Phys. Chem. Chem. Phys.* **2005**, *7*, 3297.
[65] R. Ahlrichs, M. Bär, M. Häser, H. Horn, C. Kölmel, *Chem. Phys. Lett.* **1989**, *162*, 165.
[66] K. Wolinski, J. F. Hinton, P. Pulay, *J. Am. Chem. Soc.* **1990**, *112*, 8251.
[67] T. Helgaker, P. Jørgensen, *J. Chem. Phys.* **1991**, *95*, 2595.
[68] M. J. Frisch, G. W. Trucks, H. B. Schlegel, G. E. Scuseria, M. A. Robb, J. R. Cheeseman, G. Scalmani, V. Barone, B. Mennucci, G. A. Petersson, H. Nakatsuji, M. Caricato, X. Li, H. P. Hratchian, A. F. Izmaylov, J. Bloino, G. Zheng, J. L. Sonnenberg, M. Hada, M. Ehara, K. Toyota, R. Fukuda, J. Hasegawa, M. Ishida, T. Nakajima, Y. Honda, O. Kitao, H. Nakai, T. Vreven, J. A. Montgomery, Jr., J. E. Peralta, F. Ogliaro, M. Bearpark, J. J. Heyd, E. Brothers, K. N. Kudin, V. N. Staroverov, R. Kobayashi, J. Normand, K. Raghavachari, A. Rendell, J. C. Burant, S. S. Iyengar, J. Tomasi,

M. Cossi, N. Rega, J. M. Millam, M. Klene, J. E. Knox, J. B. Cross, V. Bakken, C. Adamo, J. Jaramillo, R. Gomperts, R. E. Stratmann, O. Yazyev, A. J. Austin, R. Cammi, C. Pomelli, J. W. Ochterski, R. L. Martin, K. Morokuma, V. G. Zakrzewski, G. A. Voth, P. Salvador, J. J. Dannenberg, S. Dapprich, A. D. Daniels, Ö. Farkas, J. B. Foresman, J. V. Ortiz, J. Cioslowski, D. J. Fox, Gaussian 09, Revision A.02, Gaussian, Inc.: Wallingford, CT, **2009**.

[69] A. D. Becke, *J. Chem. Phys.* **1993**, *98*, 1372.

[70] C. Lee, W. Yang, R. G. Parr, *Phys. Rev. B: Condens. Matter Mater. Phys.* **1988**, *37*, 785.

[71] A. Schäfer, H. Horn, R. Ahlrichs, *J. Chem. Phys.* **1992**, *97*, 2571.

[72] S. Miertuš, E. Scrocco, J. Tomasi, *Chem. Phys.* **1981**, *55*, 117.

[73] J. Tomasi, B. Mennucci, R. Cammi, *Chem. Rev.* **2005**, *105*, 2999.

[74] G. Scalmani, M. J. Frisch, *J. Chem. Phys.* **2010**, *132*, 114110.

[75] DALTON 2011, *A Molecular Electronic Structure Program*, 2011, available at: http://www.daltonprogram.org.

[76] C. Wang, M. Straka, P. Pyykkö, *Phys. Chem. Chem. Phys.* **2010**, *12*, 6187.

[77] A. Bagno, M. Bonchio, J. Autschbach, *Chem. Eur. J.* **2006**, *12*, 8460.

[78] S. Standara, K. Maliňáková, R. Marek, J. Marek, M. Hocek, J. Vaara, M. Straka, *Phys. Chem. Chem. Phys.* **2010**, *12*, 5126.

[79] S. Standara, K. Bouzková, M. Straka, Z. Zacharová, M. Hocek, J. Marek, R. Marek, *Phys. Chem. Chem. Phys.* **2011**, *13*, 1.

[80] A. Bagno, F. Rastrelli, G. Saielli, *J. Org. Chem.* **2007**, *72*, 7373.

Received: 13 March 2013
Revised: 17 April 2013
Accepted: 19 April 2013
Published online on